

# A Deterministic Method for Obtaining Large-Bandwidth Frequency Combs in Microresonators with Thermal Effects

Zhen Qi<sup>1</sup>, José Jaramillo-Villegas<sup>2</sup>, Giuseppe D’Aguanno<sup>1</sup>, Thomas F. Carruthers<sup>1</sup>, Omri Gat<sup>3</sup>, Andrew M. Weiner<sup>4</sup>, and Curtis R. Menyuk<sup>1</sup>

1. University of Maryland at Baltimore County, 1000 Hilltop Circle, Baltimore, MD 21250, USA

2. Technological University of Pereira, Cra. 27 10-02, Pereira, Risaralda 660003, Colombia

3. Hebrew University of Jerusalem, Jerusalem 91904, Israel

4. Purdue University, West Lafayette, IN 47907, USA

zhenqi1@umbc.edu

**Abstract:** We describe a deterministic method for obtaining large-bandwidth frequency combs in microresonators using cnoidal waves in the soliton crystal limit. We take thermal effects into account. © 2020 The Author(s)

**OCIS codes:** 190.0190, 140.0140.

High- $Q$  optical microresonators with a Kerr nonlinearity that are pumped by continuous-wave (CW) laser light can produce frequency combs that have important potential applications to metrology and high-resolution spectroscopy [1, 2]. However, these frequency combs, which are typically generated by a single soliton pulse in the microresonator, are difficult to obtain deterministically. They are usually obtained through a quasi-random process in which the pump frequency detuning with respect to a cavity resonance is repeatedly swept until a soliton appears at the end of one of the sweeps. Recently, single solitons and more generalized periodic structures—cnoidal waves—have been extensively studied [3–6]. A cnoidal wave of periodicity  $N$  is a waveform that repeats  $N$  times in one round trip in the microresonator. In contrast to single solitons, which correspond to cnoidal waves of periodicity 1, higher-periodicity cnoidal waves are typically easier to access and use the pump more efficiently.

In the process of generating single solitons and other cnoidal waves, the cavity power varies, and the temperature of the microresonator changes. The temperature change leads to a change in the index of refraction, which shifts the cavity resonance and hence the pump frequency detuning. As a result, single solitons are thermally unstable and when generated can quickly disappear unless they are actively stabilized [7–9].

In this work, we describe a deterministic method for obtaining large-bandwidth frequency combs, taking into account thermal effects. Our method relies on first obtaining a narrow-bandwidth cnoidal wave with a large pedestal whose peaks are periodically spaced. By then simultaneously and adiabatically increasing the frequency detuning and the pump amplitude in an appropriate ratio, so that the cnoidal wave remains stable, it gradually transforms into a stable soliton crystal whose peaks are periodically spaced due to the way in which it was created. We are building on prior work in which we described this process but neglected thermal effects [5]. Thermal effects play a critical role in waveform formation in microresonators. Hence, this work is the first to demonstrate that our deterministic method is feasible in practice.

We start with the generalized Lugiato-Lefever equation (LLE), which after normalization becomes [9]

$$\frac{\partial \psi}{\partial t} = i \frac{\partial^2 \psi}{\partial x^2} + i|\psi|^2 \psi - [1 + i(\alpha + \Phi)] \psi + F, \quad (1)$$

$$\frac{\partial \Phi}{\partial t} = AP - B\Phi, \quad (2)$$

where  $\psi$  is the slowly varying envelope of the electric field,  $t$  is time,  $x$  is the azimuthal coordinate,  $\alpha$  is the detuning of the stimulated cavity resonance from the pump laser at the ambient temperature,  $\Phi$  is the thermal detuning, and  $F$  is the pump amplitude. We have  $-L/2 \leq x \leq L/2$ , where  $L$  is the mode circumference normalized with respect to the dispersive scale length. In Eq. (2), the parameter  $P = (1/L) \int_{-L/2}^{L/2} |\psi(x)|^2 dx$  is the average intracavity power, and  $A$  and  $B$  are thermal coefficients that describe the thermal shift of the resonance due to the intracavity power and thermal relaxation, respectively. We also define the ratio  $C = -A/B$  since the stationary solutions only depend on this ratio.

We calculated the stable regions in the  $\alpha$ - $F$  parameter space for the cnoidal waves up to  $N = 16$ , both without ( $C = 0$ ) and with ( $C = 5$ ) thermal effects included, setting  $L = 50$ , which corresponds approximately to the Wang et al. experiments [10]. We used the dynamical methods that are described in detail in [5]. Figs. 1(a) and (b) show the stable regions. There is a systematic shift of the stable regions to higher values of  $\alpha$  due to thermal effects.

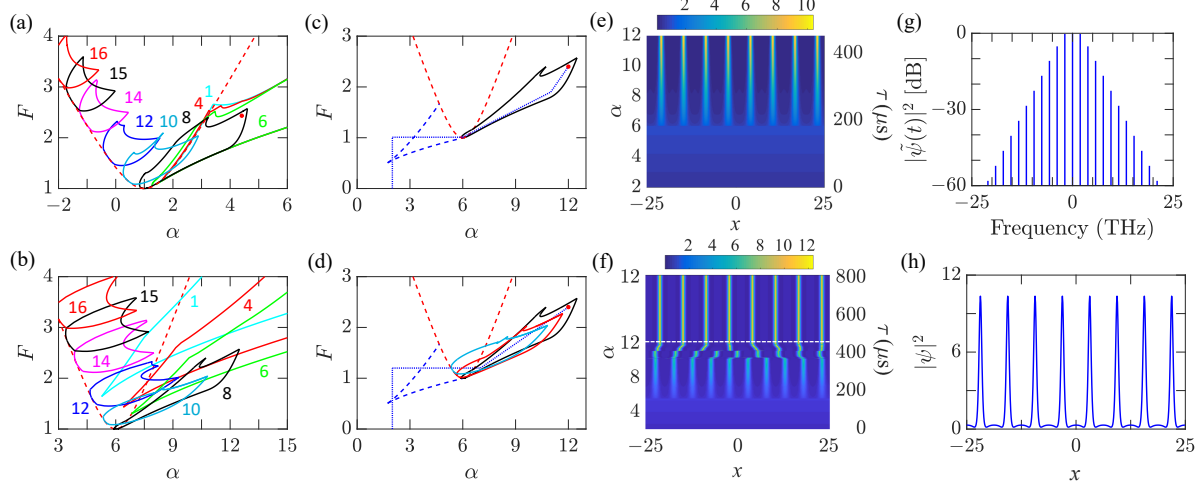


**Fig. 1.** Stable regions of cnoidal waves (a) without ( $C = 0$ ) and (b) with ( $C = 5$ ) thermal effects. We label the periodicity of the cnoidal wave regions. In (c) and (d), we show two different paths through the parameter space to obtain broad bandwidth frequency combs. The red-dashed curves in (a)-(d) show the limit above which continuous waves are unstable, and the blue-dashed curves in (c) and (d) limit the region within which continuous waves with different amplitudes are stable. The red dot at  $\alpha = 4.3, F = 12$  shows the final values at the end of the evolution. We show the evolution in (e) and (f). The white-dashed line in (f) shows the time at which we fixed  $\alpha$  and  $F$ . We show the final frequency comb and soliton crystal waveform in (g) and (h). They are the same for both paths and the same as in Figs. 5(a) and 5(b) of [5], which did not include thermal effects.

Although the map of the stable regions is qualitatively similar in both cases, there are significant quantitative differences. In particular, we see that the stable region for single solitons (labeled 1) does not overlap the stable region for higher-periodicity cnoidal waves when thermal effects are included. This result is consistent with the experimental and simulation results of Guo et al. [8] in crystalline microresonators.

Paths through the parameter space, shown as blue-dotted lines in Figs. 1(c) and (d) lead to the deterministic generation of a periodicity-8 soliton crystal. It is necessary to move sufficiently slowly through the parameter space, so that the evolution is adiabatic. In Figs. 1(e) and (f), we show the evolution for two different paths in the parameter space, ending at the point shown as a red dot. We verified that if we move at half the speed through the parameter space, the results are almost unchanged. We show the final comb spectrum in Fig. 1(g) and the corresponding waveform in Fig. 1(h). The red-dashed curves in Figs. 1(a)-(d) indicate the limit above which continuous waves are unstable. The blue-dashed curves show the limits of a region inside of which two continuous waves with different amplitudes are stable. It is necessary to enter this region through the upper blue-dashed curve in order to generate the higher-amplitude continuous wave, which then yields an 8-periodicity cnoidal wave when it becomes unstable. For the path in Fig. 1(e), we immediately obtain the periodicity-8 cnoidal wave, and the soliton crystal is well-formed by the time the path reaches the final point. By contrast, for the path in Fig. 1(f), the cnoidal wave first has periodicity-10, which leads to a transient evolution before the periodicity-8 soliton crystal emerges. We continued the evolution from time marked with the white-dashed line to ensure that the final waveform is stable as the dynamical method predicts. The final waveform and comb spectrum for both paths is exactly the same.

In conclusion, we have demonstrated that it is possible to deterministically access broadband frequency combs in microresonators with a standard configuration by adiabatically moving along paths in the (frequency detuning)  $\times$  (pump amplitude) parameter space that avoids the chaotic region. Although the map of the stable regions is qualitatively similar without and with thermal effects included, there are significant quantitative differences.

## References

1. S. A. Diddams, J. Opt. Soc. Am. B **27**, B51 (2010).
2. T. J. Kippenberg, R. Holzwarth, and S. A. Diddams, Science **332**, 555 (2011).
3. A. Coillet, I. Balakireva, R. Henriet, K. Saleh, L. Larger, J. M. Dudley, C. R. Menyuk, and Y. K. Chembo, IEEE Photon. J. **5**, 6100409 (2013).
4. Z. Qi, G. D'Aguanno, and C. R. Menyuk, J. Opt. Soc. Am. B **34**, 785 (2017).
5. Z. Qi, S. Wang, J. Jaramillo-Villegas, M. Qi, A. M. Weiner, G. D'Aguanno, T. F. Carruthers, and C. R. Menyuk, Optica **6**, 1220 (2019).
6. D. Kholmyansky and O. Gat, Phys. Rev. A **100**, 063809 (2019).
7. X. Yi, Q. -F. Yang, K. Y. Yang, M. -G. Suh, and K. Vahala, Optica **2**, 1078 (2015).
8. H. Guo, M. Karpov, E. Lucas, A. Kordts, M. H. P. Pfeiffer, V. Brasch, G. Lihachev, V. E. Lobanov, M. L. Gorodetsky, and T. J. Kippenberg, Nat. Photonics **13**, 94 (2017).
9. C. Bao, Y. Xuan, J. A. Jaramillo-Villegas, D. E. Leaird, M. Qi, and A. M. Weiner, Opt. Lett. **42**, 2519 (2017).
10. P. -H. Wang, J. A. Jaramillo-Villegas, X. Yuan, X. Xue, C. Bao, D. E. Leaird, M. Qi, and A. M. Weiner, Opt. Exp. **24**, 10890 (2016).